An analysis of out-of-band emission and in-band interference for precoded and classical OFDM systems

Medhat Mohamad*, Rickard Nilsson* and Jaap van de Beek*†
*Department of Computer Science, Electrical and Space Engineering
Luleå University of Technology, SE–97187, Luleå, Sweden.
{medhat.mohamad, rickard.o.nilsson, jaap.vandeBeek}@ltu.se
†Huawei Technologies, Sweden
{jaap.vandebeek}@huawei.com

***Abstract*—In this paper we present analytical expressions for the out-of-band (OOB) emission and in-band interference of two different OOB suppressed OFDM-systems; classical low-pass filtered and precoded. Then, we analytically compare their performance in terms of OOB emission suppression and introduced level of in-band interference. We analyse the fact that the in-band interference introduced by the filter depends on the length of the cyclic prefix as well as the behavior of the channel while that of the precoded OFDM does not. The analysis confirms that edged subcarriers suffer higher in-band interference than central subcarriers. Moreover, frequency precoders, for a specific choice of notching frequencies, can outperform time precoders.**

I. Introduction

One of the few drawbacks with traditional OFDM is its relative high levels of out-of-band (OOB) emission which results in strong interference into neighbouring frequency bands. This plays a crucial role in the legitimacy of OFDM in the coming communication systems and standards especially with the cognitive radio where many different radio-systems must be able to co-reside politely in densely packed spectrum bands.

One track is to replace the whole OFDM system with lower OOB emission systems such as the filter bank multicarrier (FBMC) or the universal filtered multicarrier (UFMC) [1]–[3]. Although those techniques show impressive results at the level of supression of OOB emission, yet their drawbacks appear in implementation complexity issues as well as their degraded performance in MIMO channels.

On the other track, suppression of the OOB emission can be done by processing the plain OFDM signal. This is done by either treating the OFDM signal after modulation (low pass filtering and windowing) or before modulation (carrier cancellation and precoding) [4].

While any of these approaches can be efficient in suppressing the OOB emission, all of them inevitably comes with a certain price. Carrier cancellation is spectrally inefficient due to sacrificing of subcarriers. Filtering and windowing introduce in-band interference by smearing the OFDM signal to suppress the OOB emission. Precoding introduces ICI by linearly combining the independent data symbols.

Many precoding schemes are presented in the literature. In [5], OOB emission are suppressed by modulating the subcarriers with well-chosen precoded data symbols. In [6] the main goal is to push the OFDM signal continuous in time, as well as its N-derivatives by forcing the edges of the OFDM symbol to zero. In [5], the main goal is to introduce nulls at well chosen frequencies in the OFDM spectrum. In [7] the constraints on the precoding matrix suggested in [5] are relaxed. In [8], the precoder is designed to limit the OOB emission suppressed below a particular power mask.

A comparison between the different schemes regarding the OOB emission suppression is carried out [4]. Yet, to our knowledge, no comparison at the level of the *in-band interference* introduced by the different schemes has been carried out.

In this paper, we focus on the two precoding approaches presented in [6] and [7] respectively and compare them with the classical OFDM (we refer to the low pass filtered OFDM as classical OFDM). We present *analytical expressions* for the introduced in-band interference at different subcarriers in both cases. Then, we make a *comparative analysis* of the OOB emission suppression performance and the amount of in-band interference. We investigate the effect of the channel behaviour as well as the length of the cyclic prefix on the in-band interference level. We also discuss the fact that in both cases edge subcarriers are more affected by interference than centrally located subcarriers. and finally, we support our analytical results with simulations of the bit error rate (BER).

In Section II, we describe the two different OOB suppression approaches: classical and precoded OFDM. In section III, we derive analytical expressions of the in-band interference for the two approaches. We check the effect of cyclic prefix length on the level of in-band interference introduced. In section IV, we analyse and compare the OOB suppression performance and in-band interference effect for both precoded and classical OFDM under different channels behaviour. Finally, we summarize our work in Section V.

II. Out-of-band emission suppression

We will investigate the baseband OFDM transmitted signal, given by

$$s(t) = \sum_{i=-\infty}^{\infty} s_i(t - i(T_s + T_g)), \tag{1}$$

where T_s is the symbol duration, T_g is the duration of the cyclic prefix and $s_i(t)$ is the i^{th} OFDM transmitted symbol represented by $s_i(t) = \sum_{k=0}^{K-1} d_{k,i} e^{-j2\pi \frac{k}{T_s} t}, \quad -T_g \leq t \leq T_s$. Here, $d_{k,i}$ represents an information symbol taken from some

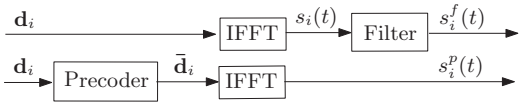

Fig. 1. OFDM system model with a filter (top) or a precoder (bottom) used for the suppression of out-of-band emission.

symbol constellation $\mathcal{C}$ where $k \in [0, 1, ..., K-1]$ represents the subcarrier index.

The power spectrum of the OFDM signal (1) is [7]

$$S(f) = \frac{1}{T}||\mathbf{a}(f)||_2^2, \tag{2}$$

where $\mathbf{a}(f)$ is a vector collecting the modulated subcarriers in the frequency domain such that

$$\mathbf{a}(f) = [a_0(f), a_1(f) \dots a_{K-1}(f)]^T, \tag{3}$$

and $a_k(f)$ is the k^{th} modulated subcarrier given by

$$a_k(f) = Te^{-j\pi(T_s-T_g)(f-\frac{k}{T_s})}\text{sinc}(\pi T(f - \frac{k}{T_s})), \tag{4}$$

where $T = T_s + T_g$. As is well known, the spectrum (2) decays with $1/f^2$.

In what follows, we study the suppression of OOB emission of signal (1) by a classical approach and a precoding approach.

A. Classical approach

The first approach we study applies a low pass filter to (1) to suppress the OOB emission as shown in Figure 1 (top). Assuming that the filter has impulse response $h(t)$ with length T_h and support on $[0, T_h]$, then after introducing symbol $s_i(t)$ into the filter, the i^{th} classical filtered output symbol is

$$s_i^f(t) = s_i(t) * h(t), \tag{5}$$

and the power spectrum of the classical signal becomes

$$S^f(f) = |H(f)|^2 S(f), \tag{6}$$

where $H(f)$ is the frequency response of the filter (the Fourier transform of the impulse response of the filter). The spectrum of a classical OFDM system is reperesented in Figure 3.

The classical baseband transmitted signal $s^f(t)$ will be longer than the baseband transmitted signal $s(t)$ since the filtering process extends the length of the output signal. If the length of the cyclic prefix is not long enough to mitigate the joint dispersion caused by the filter and the channel impulse response, the following OFDM symbol is affected by ISI. Figure 2 illustrates this situation. It shows the tail of the impulse response from symbol s_{i-1} that is not absorbed by the cyclic prefix, thus causing interference with the following OFDM symbol s_i. In section III we show how much ISI will affect the OFDM symbols subcarriers.

B. Precoding approach

A second recent approach for suppressing the OOB emission is through precoding of the symbols that modulate the subcarriers. Controlled weights are added to our data symbols before modulating the subcarriers. This is illustrated in Figure 1 (bottom). Naturally, those weights will cause distortion in the OFDM system.

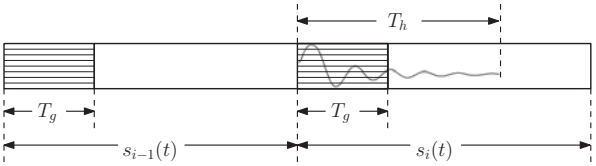

Fig. 2. ISI of symbol $s_{i-1}(t)$ on symbol $s_i(t)$. The cyclic prefix of length T_g mitigates part of the filter's impulse response of length T_h but the remaining part will interfere with the following OFDM symbol.

The i^{th} precoded OFDM symbol is

$$s_i^p(t) = \sum_{k=0}^{K-1} \bar{d}_{k,i} e^{-j2\pi \frac{k}{T_s} t}, \quad -T_g \le t \le T_s, \tag{7}$$

where $\bar{\mathbf{d}}_\mathbf{i} = [\bar{d}_{1,i}, \bar{d}_{2,i}, \dots, \bar{d}_{K-1,i}]^T$ is the linearly precoded data symbol vector such that

$$\bar{\mathbf{d}}_i = \mathbf{G}\mathbf{d}_i, \tag{8}$$

where $\mathbf{d}_\mathbf{i} = [d_{1,i}, d_{2,i}, \dots, d_{K-1,i}]^T$ and $\mathbf{G}$ is the precoding matrix given by [6], [7]

$$\mathbf{G} \triangleq \mathbf{I} - \mathbf{B}^H(\mathbf{B}\mathbf{B}^H)^{-1}\mathbf{B}. \tag{9}$$

The precoding matrix $\mathbf{G}$, then, is the projection onto the nullspace $\mathcal{N}(\mathbf{B})$ of $\mathbf{B}$. The choice of $\mathbf{B}$ depends on the precoding technique followed. We recall two choices from the literature here.

In the time precoding approach proposed in [6], the OOB emission are treated by managing the discontinuity property of the OFDM signal. In [6], the OOB emission are suppressed by rendering the OFDM signal represented by (1) as well as its first N derivatives continuous by pushing the beginning and the end of the OFDM symbol to the origin, *i.e.*

$$\frac{d^n}{dt^n} s_i^p(t)\Big|_{t=-T_g} = \frac{d^n}{dt^n} s_i^p(t)\Big|_{t=T_s} = 0. \tag{10}$$

This is accomplished by choosing $\mathbf{B}$ in (9) as

$$\mathbf{B} \triangleq \begin{bmatrix} \mathbf{A}\mathbf{\Phi} \\ \mathbf{A} \end{bmatrix}, \tag{11}$$

where $\mathbf{A}$ is an $(N+1) \times K$ matrix with entries $[\mathbf{A}]_{ij} = {k_j}^i$, $i = 0 \dots N$, $j = 0 \dots K-1$ and $\mathbf{\Phi} = \text{diag}(e^{j2\pi k_0}, e^{j2\pi k_1} \dots e^{j2\pi k_{K-1}})$ [6].

In the frequency precoding approach proposed in [7], the core idea falls in nulling the spectrum of $s(t)$, $S(f)$, at certain set of frequencies, $\mathcal{M} = \{f_0 \dots f_m \dots f_{M-1}\}$, such that $S(f_m) = 0$. Here, the frequency precoder, $\mathbf{B}$ is an $M \times K$ matrix collecting the notching vectors at different notching frequencies.

$$\mathbf{B} = [\mathbf{a}(f_0) \dots \mathbf{a}(f_m) \dots \mathbf{a}(f_{M-1})]^T, \tag{12}$$

where $\mathbf{a}(f_m)$ is the subcarriers vector at frequency f_m as defined in (4).

For both the time precoder and the frequency precoder, the precoded OFDM spectrum is given by [7]

$$S^p(f) = \frac{1}{T}||\mathbf{G}^T\mathbf{a}(f)||_2^2, \tag{13}$$

where $\mathbf{G}$ is defined either through (11) or (12). Figure 3 shows a precoded OFDM spectrum for both N-continuous time precoder and frequency precoder.

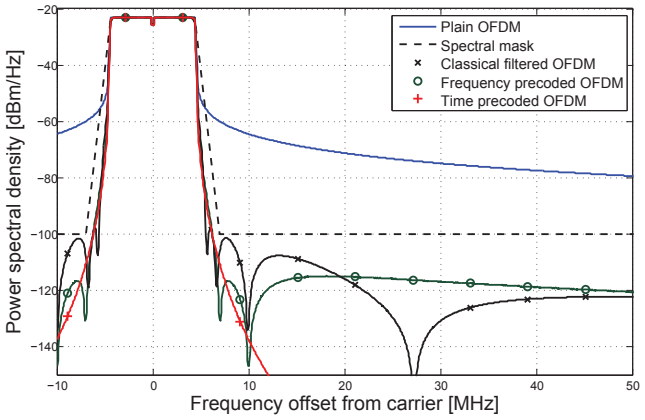

Fig. 3. Power spectral densities of (plain, 8^{th} ordered Chebyshev II classical filtered, frequency precoded with 8 notching frequencies, and 6-continuous time precoded) OFDM systems. The out-of-band emission are suppressed below the spectral mask.

III. IN-BAND INTERFERENCE ANALYSIS

Both the classical and the precoding approaches cause a loss of orthogonality between subcarriers, and hence in-band interference. Since this interference will affect the bit error rate (BER) at the receiver side, we analyse interference here. While [6] and [7] show the *total* interference power introduced by time and frequency precoders, here we extend these results by analysing the interference in each particular subcarrier and study the interference introduced by filtering.

A. Classical interference

To estimate the classical filtering interference, the approach used in [9] is useful. While [9] analyses the interference introduced into OFDM system due to the excess of the length of the *channel* over that of the cyclic prefix, here, we use the fact that the nature of the interference produced by the filter is similar to that of the channel. We derive the interference for the continuous-time model represented in (5).

The ISI from symbol $s_{i-1}^f(t)$ that affects symbol $s_i^f(t)$ is

$$q_i(t) = \int_{\tau=T_g+t}^{T_h} h(\tau) s_{i-1}(t-\tau) d\tau, \quad 0 \le t \le T_h - T_g, \quad (14)$$

provided that the classical filtered OFDM symbol affects only the immediately succeeding OFDM symbol, $T_h \le T_s$.

Since the amount of interference the ISI causes on each subcarrier is the subject of study of this paper, we evaluate the power spectral density of the ISI (see also [9]). The ISI on the system's subcarriers is given by the Fourier transform of (14) evaluated at the frequencies $f = \frac{k}{T_s}$,

$$\begin{aligned} Q_i(k) &= \int_0^{T_s} q_i(t) e^{-j2\pi \frac{k}{T_s} t} dt, \\ &= \int_0^{T_s} \int_{\tau=T_g+t}^{T_h} h(\tau) s_{i-1}(t-\tau) e^{-j2\pi \frac{k}{T_s} t} d\tau dt, \end{aligned} \quad (15)$$

for $k = 0, 1, \ldots, K-1$.

Assuming that the data symbols are uncorrelated, the power spectral density of the interference then becomes

$$D_{\text{ISI}}(k) \triangleq E\{Q_i(k) Q_i^*(k)\} = \sigma^2 \int_{T_g}^{T_h} |H_k(t)|^2 dt, \quad (16)$$

where $H_k(t)$ is the Fourier transform of the tail of the filter's impulse response defined as

$$H_k(t) \triangleq \int_{\tau=t}^{T_h} h(\tau) e^{-j2\pi \frac{k}{T_s} \tau} d\tau, \quad (17)$$

and σ^2 is the average power of the modulated data symbols d_k.

In [9], it has been also proven that the spectral density of the inter-carrier interference (ICI) is *the same* as that of the ISI. Therefore, the total spectral interference on the k^{th} subcarrier due to filtering is

$$\boxed{D_{\text{total}}^f(k) = 2 D_{\text{ISI}}(k).} \quad (18)$$

To examine the distortion level introduced due to classical filtering, We adopt an OFDM system complying with 3GPP E-UTRA/LTE specifications [10] of sampling time $T_s = \frac{1}{15}$ ms, 9 MHz bandwidth, 600 subcarriers (*i.e.* 15 kHz spacing between the adjacent subcarriers) and a guard time interval $T_g = \frac{3}{640}$ ms $\approx 4.7\mu$s. We assume *a 1-tap channel* and check the relative interference power of the filter for different lengths of the cyclic prefix.

We adopt a Chebyshev type II filter in our discussion and analysis. In [11] it was concluded that the this filter outperforms other types of filters, generating the least ISI energy under identical complexity constraints compared with other filter types. Yet, the analysis here can be generalized for any other types of filters.

In Figure 4, we see that for the cyclic prefix length given by LTE standards (4.7μs), we get the lowest distortion performance (under the assumption of a 1-tap channel). Figure 4 also shows that the relative interference level increases as the length of the cyclic prefix decreases especially at central subcarriers.

B. Precoding interference

The *total* interference power for the time precoder is $2N+2$ and for the frequency precoder is M (see [6] and [7] respectively). These results show that the interference power of the frequency precoder and the time precoder is directly related to the number of constraints on $\mathbf{B}$ matrix. For the time precoder, increasing the degree of continuity (*i.e.* increase the derivative order) will suppress more OOB emission at the cost of increasing total interference as well as the interference per each subcarrier. For the frequency precoder increasing the number of notching frequencies will also reduce the OOB emission at the cost of increasing the interference. But how much is the in-band interference *at each subcarrier*?

For the precoder we define the in-band interference vector

$$\mathbf{w_i} \triangleq \mathbf{d_i} - \bar{\mathbf{d}}_\mathbf{i} = \mathbf{B}^H (\mathbf{B}\mathbf{B}^H)^{-1} \mathbf{B} \mathbf{d_i} = \mathbf{P} \mathbf{d_i}, \quad (19)$$

where $\mathbf{P} = \mathbf{B}^H (\mathbf{B}\mathbf{B}^H)^{-1} \mathbf{B}$ is the projection matrix of $\bar{\mathbf{d}}_\mathbf{i}$ onto the orthogonal complement of the nullspace $\mathcal{N}(\mathbf{B})$ of $\mathbf{B}$.

The power of the interference throughout the subcarriers is collected in $[\mathbf{\Theta}]_{kk}$ where $\mathbf{\Theta}$ is defined as

$$\mathbf{\Theta} \triangleq E\{\mathbf{w_i} \mathbf{w_i}^H\} = \mathbf{P} E\{\mathbf{d_i} \mathbf{d_i}^H\} \mathbf{P}^H. \quad (20)$$

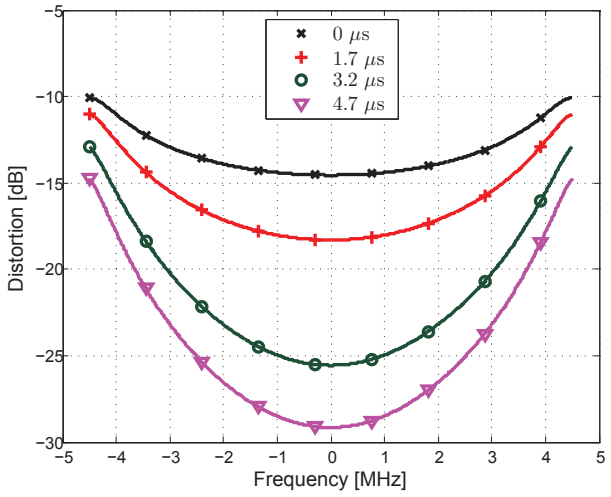

Fig. 4. Classical filtering interference (18) (relative to the subcarriers power) with different lengths of the cyclic prefix (number of subcarriers = 600).

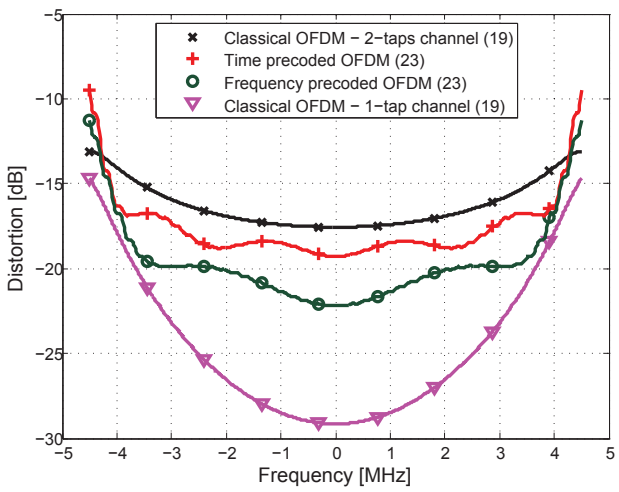

Fig. 5. In-band intereference (18) (relative to the subcarriers power) for the OFDM signals in Figure 3 due to 8^{th} order Chebyshev II filter (1-tap and 2-taps channels) , and (22) due to precoding with 8 notching frequencies-frequency precoder, and 6-continuous time precoder.

Under the assumption that symbols $\mathbf{d_i}$ are uncorrelated, $E\{\mathbf{d_i}\mathbf{d_i}^H\} = \mathbf{I}$, (20) becomes

$$\mathbf{\Theta} = \mathbf{P}\mathbf{P}^H = \mathbf{P}. \tag{21}$$

From (21) we find the interference power at each subcarrier on the diagonal of $\mathbf{P}$, *i.e.*

$$\boxed{D^p_{\text{total}}(k) = [\mathbf{P}]_{kk}.} \tag{22}$$

From (22), we can see that the in-band interference introduced due to precoding is *indpendent* on the length of the cyclic prefix.

It is noteworthy to mention that for the frequency precoder, the choice of the notching frequencies set, $\mathcal{M}$, plays a critical rule on the amount of emission suppressed, on the shape of the precoded OFDM spectrum, as well as the amount of interference introduced at *each subcarrier* (yet, the *total amount* of interference in OFDM symbol is only related to the number of the notching frequencies but not their location). The choice of the optimal notching frequencies $\mathcal{M}$ is still subject of research and beyond the scope of this paper.

IV. Comparative Analysis of In-Band Interferences (18) and (22)

In this section, we compare the in-band interferences (18) and (22) by revisiting the OFDM system adopted in Figures 3 and 4. We concentrate our study regarding three aspects: distortion level, capacity performance and BER.

Since for cognitive radio technology we need a very low OOB emission, our requirement then is to suppress the OOB emission more than 77 dB at 150% of the bandwidth (*i.e.* 35 dB lower than the spectral mask specified by LTE) . This is represented by the spectral mask shown in Figure 3. To achieve that at least an 8^{th} order Chebyshev II filter, a 6-continuous time precoder ($N = 6$) or a frequency precoder of 8 notching frequencies ($M = 8$) is required. For the frequency precoder, the spectrum is notched at -10001 kHz, -10000 kHz,-7001 kHz, -7000 kHz, 7000 kHz, 7001 kHz, 10000 kHz and 10001 kHz. Under these conditions, we can make a fair investigation of the level of interference each system presents.

As described in Figure 2 and analysed in Figure 4 (for 1-tap channel), if the length of the channel impulse response is shorter than the length of the cyclic prefix, the cyclic prefix will absorb part of the interference introduced by the filter. Therefore, the behaviour of the channel plays a crucial rule on the level of in-band interference. In this analysis we assume two channel behaviours: 1- a 1-tap channel *i.e.* the full cyclic prefix is dedicated to mitigate the ISI introduced by the filter. 2- two equal taps channel separated by 4.7μs *i.e.* the full cyclic prefix is dedicated to mitigate the ISI of the channel.

Figure 5 shows the in-band interferences (18) and (22). The interference of the frequency precoder is approximately 3 dB better than that of the time precoder. The interference introduced by the filter dramatically changes under the influence of the channel's behaviour. For 1-tap channel the interference of the filter is lower than those of the two precoders. While for the 2-taps channel the precoders performance is superior. On the other hand, the length of the channel has no effect on the precoding distortion level.

Both in-band interferences (18) and (22) are higher at the edges (especially (22)) and decreases toward the center. Since OOB power leaking from edged subcarriers is higher than that of central subcarriers, edge subcarriers will face higher emission suppression and therefore, will get higher in-band interference.

Figure 6 shows the average capacity performance per OFDM subcarrier for classical (in 1-tap and 2-taps channel scenarios) and precoded OFDM systems compared to original plain OFDM system. The capacity performance for the classical and precoded systems is near that for the plain OFDM system at signal to noise ratio (SNR) less than 3 dB. The performance of the precoded as well as the (2-taps channel) classical system start to degrade away from that of the plain system as the SNR starts to increase. Yet, for the 1-tap channel, the capacity performance stays very similar to that of the plain OFDM. For the precoders, although, both frequency and time precoded systems appear to have very close capacity performance but still the frequency precoded system supercedes that of the time

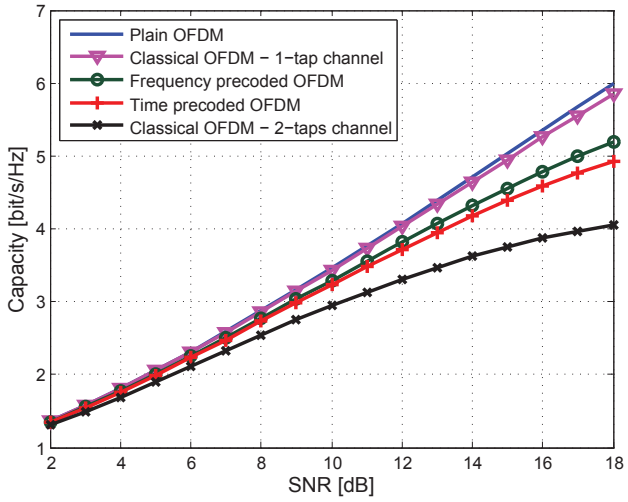

Fig. 6. Capacity performance of 8 notches frequency precoded, 6-continuous time precoded and 8^{th}-order Chebyshev II classical filtered (with 1-tap and 2-taps channel) OFDM system with 600 subcarriers compared to plain OFDM system.

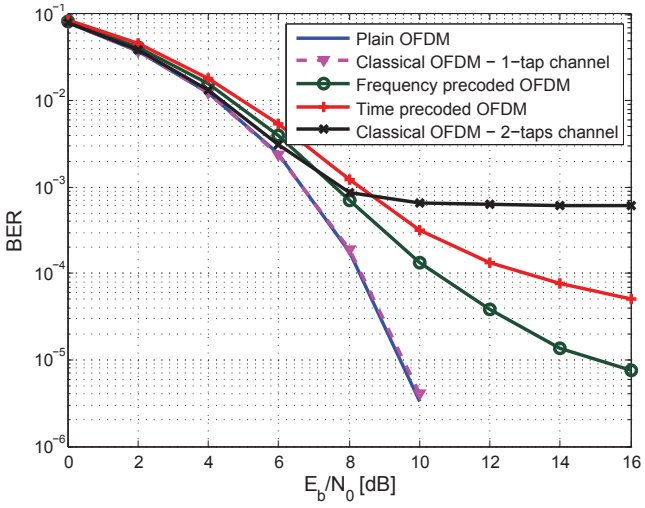

Fig. 7. BER of plain, 8 notches frequency precoded, 6-continuous time precoded and 8^{th}-order Chebyshev II classical filtered (with 1-tap and 2-taps channel) 600 subcarriers OFDM, QPSK system in AWGN.

precoded system.

Finally, we support our analytical results with BER curves simulations presented in Figure 7. We choose a QPSK mapped symbols to be modulated over the OFDM system defined above. We assume no knowledge of the precoding (or filtering) at the receiver side.

The results show that for the 1-tap channel (when the cyclic prefix is compensating most of the in-band interference effect of the filter), the BER performance of the classical OFDM is very similar to that of plain OFDM. The result degrades extensively with the 2-taps channel (when the full length of the cyclic prefix is dedicated to get rid of the channel ISI) where the curve drift away from the typical system after 6 dB SNR. On the other hand, we can see that the performance of the precoding techniques falls between the two classical cases. We can also notice that for this particular choice of notching frequencies, the frequency precoder performance of this OFDM setup is superior over that of the time precoder performance.

V. CONCLUSIONS

We hold analytical comparison between two OFDM OOB emission suppresion approaches: classical low pass filtering and precoding. We provide closed form expressions of the suppressed spectrum as well as the in-band interference introduced by the two approaches. For the classical case, we prove the dependency of the in-band interference on the cyclic prefix length as well as the behaviour of the channel. This can dramatically increase or decrease the in-band interference level. Precoders' interference on the other hand is independent on the length of the cyclic prefix and channel behaviour. Our analysis shows that for this introduced spectrum and special choice of notching frequencies, frequency notching precoder appears to outperform the N-continuity time precoder. We also confirm the claim that the interference is larger at the edged subcarriers and decreases towards the central subcarriers.

ACKNOWLEDGMENT

We gratefully acknowledge that the work in this contribution was carried out with financial support from the Swedish Research Council, grant nr 2014-5977.

REFERENCES

[1] B. Farhang-Boroujeny, "OFDM versus filter bank multicarrier," *Signal Processing Magazine, IEEE*, vol. 28, no. 3, pp. 92–112, 2011.

[2] V. Vakilian, T. Wild, F. Schaich, S. ten Brink, and J.-F. Frigon, "Universal-filtered multi-carrier technique for wireless systems beyond lte," in *Globecom Workshops (GC Wkshps), 2013 IEEE*, pp. 223–228, IEEE, 2013.

[3] G. Wunder, P. Jung, M. Kasparick, T. Wild, F. Schaich, Y. Chen, S. ten Brink, I. Gaspar, N. Michailow, A. Festag, *et al.*, "5GNOW: non-orthogonal, asynchronous waveforms for future mobile applications.," *IEEE Communications Magazine*, vol. 52, no. 2, pp. 97–105, 2014.

[4] Z. You, J. Fang, and I.-T. Lu, "Out-of-band emission suppression techniques based on a generalized ofdm framework," *EURASIP Journal on Advances in Signal Processing*, vol. 2014, no. 1, pp. 1–14, 2014.

[5] I. Cosovic, S. Brandes, and M. Schnell, "Subcarrier weighting: a method for sidelobe suppression in OFDM systems," *IEEE Communications Letters*, vol. 10, no. 6, pp. 444–446, 2006.

[6] J. van de Beek and F. Berggren, "EVM-constrained OFDM precoding for reduction of out-of-band emission," in *Vehicular Technology Conference Fall (VTC 2009-Fall), 2009 IEEE 70th*, pp. 1–5, IEEE, 2009.

[7] J. van de Beek, "Sculpting the multicarrier spectrum: a novel projection precoder," *IEEE Communications Letters*, vol. 13, no. 12, pp. 881–883, 2009.

[8] A. Tom, A. Sahin, and H. Arslan, "Mask compliant precoder for OFDM spectrum shaping," *IEEE Communications Letters*, vol. 17, no. 3, pp. 447–450, 2013.

[9] W. Henkel, G. Tauböck, P. Ödling, P. O. Börjesson, and N. Petersson, "The cyclic prefix of OFDM/DMT-an analysis," in *Broadband Communications, 2002. Access, Transmission, Networking. 2002 International Zürich Seminar on*, pp. 22–1, IEEE, 2002.

[10] *Physical Channels and Modulation (Release 8),* 3GPP TSG RAN TS 36.211, v8.4.0., Sep. 2008. [Online]. Available: http://www.3gpp.org/.

[11] M. Faulkner, "The effect of filtering on the performance of OFDM systems," *Vehicular Technology, IEEE Transactions on*, vol. 49, no. 5, pp. 1877–1884, 2000.